THE ASTROPHYSICAL JOURNAL, 360:490–503, 1990 September 10


# AN ASYMPTOTIC GIANT BRANCH STAR SURVEY IN THE SMALL MAGELLANIC CLOUD[1]

NEILL REID AND JEREMY MOULD
California Institute of Technology
*Received 1989 November 6; accepted 1990 March 2*

## ABSTRACT

We present photographic $V$- and $I$-band photometry of a 0.8 deg$^2$ region in the Small Magellanic Cloud. We have used the $V-I$ color index to identify the candidate asymptotic giant branch (AGB) stars in this field and have obtained spectroscopic observations of all of the latter with $M_{bol} < -5.5$. The majority prove to be of spectral type K4 or K5 with only one C star in the sample. We suggest that these earlier type giants are young, massive supergiants formed within the last few million years. A comparison with the LMC shows that the two systems have nearly identical AGB luminosity functions, suggesting that the relative star formation rates have been similar. Finally, while our radial velocity data show the well-known bimodal distribution, the width of the giant branch in the color-magnitude diagram suggests that the depth of the SMC along the line of sight is only $\sim 5$ kpc.

*Subject headings:* galaxies: Magellanic Clouds — galaxies: stellar content — luminosity function — stars: late-type

## I. INTRODUCTION

The study of luminous stars—both main-sequence and evolved—in the Galaxy is complicated by their low volume density and consequent scarcity within the solar neighborhood. With the distance to the Magellanic Clouds known with relatively high accuracy, and with all stars at effectively the same distance, these systems have provided excellent laboratories for the study of intermediate- and high-mass stars. While the absolute values of the distances to both SMC and LMC are still subject to some debate—although the uncertainties may be as little as $\pm 10\%$ for the latter—the relative distances of stars in these systems are better determined than is the case for Galactic stars, and recent years have seen numerous theoretical and observational studies of star formation in these companion galaxies. This is particularly true for stars on the asymptotic giant branch. Such stars can achieve substantial luminosities, up to $M_{bol} = -7.2$, with evolution through the double-shell-burning phase accompanied by substantial mass loss, and since most stars in the mass range $\sim 1$ to $\sim 7\ M_\odot$ become AGB stars, their behavior is important both for the chemical and for the luminosity evolution of stellar systems.

Blanco, McCarthy, and Blanco (1980) were the first to point out the discrepancy between the predictions of the then current theoretical models and the observations of the carbon star luminosity function in the Clouds. Mould and Aaronson (1982, 1986) further showed that dredge-up occurred sooner than expected among the AGB stars in the Magellanic clusters and that in the younger clusters, the AGB terminated at a lower luminosity than one would predict from the turn-off mass. Subsequent studies have reconciled theory and observation for the lower luminosity ($M_{bol} > -4.5$) stars (Iben and Renzini 1982; Lattanzio 1987). As to the absent high-luminosity giants, we have recently used *IRAS* data to search for highly obscured stars (Reid, Tinney, and Mould 1990, hereafter RTM90), and while our survey revealed few infrared sources, we did find evidence for substantial dust shells around a small number of AGB stars of only moderate luminosity, $M_{bol} \sim -5.5$. We have suggested that the final catastrophic phase of mass loss, the precursor to planetary nebula formation, is triggered before most stars acquire core masses near the Chandrasekhar limit; the almost complete absence of carbon stars with $M_{bol} < -6$ suggests that early envelope ejection happens more readily in those types of atmospheres. Thus stars are removed prematurely from the AGB, accounting for the scarcity of luminous AGB stars.

In previous papers, we have concentrated on the asymptotic giant branch stars in the LMC. In this paper we turn our attention to a region in the Small Magellanic Cloud—a lower mass, more metal-poor system with a more complex geometry. Section II describes the photographic photometry we have obtained and the photometric determination of the AGB luminosity function. In § III we present spectroscopic observations of the more luminous candidate AGB stars and we analyze these data in § IV. In § V we discuss briefly the implications of our data for the geometry of this portion of the SMC. Section VI presents our conclusion.

## II. PHOTOMETRY

### a) Plate Material and Calibration

Our study of the asymptotic giant branch stars of the Small Magellanic Cloud is based on $V$- and $I$-band photographic plates obtained using the du Pont 2.5 m telescope at Las Campanas Observatory. These plates were obtained during the same observing run (1984 October/November) as photographs of the Shapley III region of the LMC. The analysis of the latter plate material is described by Reid, Mould, and Thompson (1987, hereafter RMT87), and we shall follow a similar method in the current analysis.

Table 1 lists the plate material: three $V$-band 103a-D emulsion plates, hypered by baking in forming gas, and three infrared IV-N emulsion plates, hypered using $AgNO_3$ solution. With a plate scale of 10.′9 mm$^{-1}$, these 14 inch plates cover a total solid angle of 0.82 deg$^2$ centered on $\alpha = 1^h9^m24^s$, $\delta = -72°39'$ (equinox 1950.0). This field lies within the bay of the SMC, including part of the bar and extending east into the halo of the SMC as far as the old globular cluster Kron 68.

[1] Based on observations obtained at the Las Campanas Observatory of the Carnegie Institution of Washington.

TABLE 1

PLATE MATERIAL

| Plate | Emulsion | Exposure (minutes) | Epoch (1984) |
|---|---|---|---|
| CD 2574..... | IV N | 60 | Oct 31 |
| CD 2575..... | IV N | 60 | Oct 31 |
| CD 2581..... | IV N | 60 | Nov 1 |
| CD 2582..... | 103a-D | 15 | Nov 1 |
| CD 2584..... | 103a-D | 20 | Nov 1 |
| CD 2585..... | 103a-D | 20 | Nov 1 |

Thus there is a substantial range in the average stellar number density across the field. All the plates have been scanned using the COSMOS measuring engine at the Royal Observatory Edinburgh, and the data from the individual plates merged to give a single catalog for the field. As in our study of Shapley III, we have transformed the COSMOS magnitudes to one system (that of CD 2584 in $V$ and of CD 2581 in $I$) before deriving mean instrumental magnitudes for more than 61,000 images.

The regions near the Bar in the SMC field are relatively crowded, even at the plate scale of the 2.5 m du Pont, and in calculating the mean magnitudes it is necessary to allow for merged images. COSMOS provides some limited information on the shape of each image, notably the length of the major and minor axes of the best-fit ellipse. Following our previous experience, we have eliminated from consideration all images with an axial ratio $b/a < 0.65$. Calculating the sample completeness as a function of magnitude, the fraction of stars with at least one good measurement in both $V$ and $I$ is approximately constant at 90% for $V < 18$ and $I < 17.0$, but declines sharply at fainter magnitudes—results similar to those of the Shapley III study (RMT87, Fig. 4). Since our main aim is the study of the asymptotic giant branch, stars with $I \leq \sim 14.5$, $V \leq \sim 17$, the data are more than adequate for our purposes.

Our photometric calibration is derived from three sources. First, Azzopardi and Vigneau (1975) have published $BV$ photometry for early-type stars in the SMC, 18 of which lie within our field. Second, we have $V$- and $I$-band CCD observations made using the CTIO 4 m telescope of a field centered on NGC 416. Finally, we have used the CCD camera on the 40 inch Swope telescope at Las Campanas to obtain $VRI$ frames of two fields near NGC 416. The detector is a 512 × 320 RCA device with 25 $\mu$m pixels, giving an image scale of 0.″87 per pixel. The device has a small dark current and a significantly nonlinear response, both of which are stable and can be allowed for in the reductions. We calibrated the dark current through a series of dark exposures and computed the linearity corrections using dome flat-field frames taken with a range of exposure times. The appropriate dark current was subtracted, and the data were flat-fielded using exposures of the twilight sky.

We have used aperture photometry to determine the stellar magnitudes, choosing well-isolated stars in the NGC 416 frames. Observations of $E$-region standard stars from Graham (1982) have been used to set our CCD photometry onto the Cousins system; the passbands are well matched to the standard system, and the color terms are small. However, as is described in detail in RMT87, in calibrating the photographic photometry it is necessary to allow for a substantial color term in the $V$-band photometry. We have adopted the same approach of using the bluer stars ($V-I < 0.1$) to define the COSMOS magnitude calibration, applying the appropriate color corrections for redder stars. The residuals determined from our current observations are consistent with those found in the LMC by RMT87 (see their Fig. 2—note that the ordinate in that figure should be labeled as $[V - v]$), although with an increased number of standards we find a somewhat larger dispersion ($\pm 0.15$ mag) in the range $v - I \sim 1.0$–$2.5$ or $V-I \sim 0.5$–$1.5$. We have adopted the same color term in correcting our SMC $V$-band observations. Given the scatter about the calibration, there is some uncertainty in the zero point of the $V$ magnitudes, and colors, that we derive for evolved stars, although the relative photometry, both among SMC stars and in comparison with our LMC data, is on a more secure footing. Since our main purpose is the identification of AGB stars, this zero point uncertainty, which we estimate as $\pm 0.15$ mag, is of little importance, although see the discussion in § II*b* below. The corrections are better defined for both the early-type main-sequence stars and the redder giant stars. The dispersion about the final calibration curves is $\sim \pm 0.07$ mag at $V = 14$, rising to $\sim \pm 0.15$ at $V = 18$; $\pm 0.05$ at $I = 14$ and $\pm 0.16$ at $I = 18$. We estimate the accuracy of the transformation of the combined photometry to the standard system as better than $\pm 0.07$ in magnitude and $\pm 0.13$ in color for the bright AGB candidates discussed in this paper. The internal accuracy of the relative photometry is significantly higher.

### *b) The Color-Magnitude Diagram*

We have constructed a color-magnitude array from these calibrated photographic observations. Table 2 gives the stellar number-magnitude-color counts for the whole field surveyed, and Figure 1 presents these data for two regions within our field: a 0.18 deg$^2$ area in the low-star density eastern edge of the field, the "halo" field, and an area of half that size in the bar of the SMC. Reddening toward the SMC is relatively low: $E_{B-V} \sim 0.04$ or $E_{V-I} = 0.05$, $A_I = 0.08$ (Suntzeff *et al.* 1986). We have corrected neither the data in Table 2 nor Figure 1 for the foreground reddening. The two color-magnitude diagrams are similar in morphology, with a blue sequence due to high-mass main-sequence stars and a prominent red giant branch. As might be expected, the former feature is more prominent in the bar field with the most luminous stars at $M_I \sim 13.8$. Since $V-I \sim 0$, and adopting a distance modulus of 18.8 for the SMC (Reid and Strugnell 1986), this corresponds to $M_V \sim -5$, a mass of $M \sim 25\ M_\odot$, and an age of $\sim 8$ Myr (Maeder 1981) for the youngest stars in the field. Indeed, Figure 3 shows that the main sequence extends to brighter than $I = 13$, or $M_I < -5.8$, $M > 30\ M_\odot$.

Stars within our own Galaxy make some contribution toward the color-magnitude diagrams shown in Figure 1. As in RMT87, we have used a model to predict the number of such stars within our survey field. The model includes four disklike components: an old disk (exponential scale height perpendicular to the plane, $z_0$, 300 pc) representing stars with ages of from 1.5 to 10 Gyr, an intermediate disk ($Z_0 = 250$ pc, $\tau \sim 0.1$–$2$ Gyr), a young disk ($z_0 = 100$ pc, $\tau < 0.1$ Gyr), and an extended disk ($z_0 = 1000$ pc). These four components, which should be regarded as convenient parameterizations rather than separate populations, are all assumed to have luminosity functions of the same shape, with the appropriate high-mass cutoff. We have used the local stellar luminosity function compiled by Reid (1987) in the model, scaling the densities by factors of 0.85, 0.14, 0.01, and 0.015, respectively. Finally, we have included a spheroidal halo population, with an M3-like color-

TABLE 2

SMC COLOR-MAGNITUDE DIAGRAM

| | $V-I$ | | | | | | | | | | | | | | |
|---|---|---|---|---|---|---|---|---|---|---|---|---|---|---|---|
| $V$ | −0.3 | −0.1 | 0.1 | 0.3 | 0.5 | 0.7 | 0.9 | 1.1 | 1.3 | 1.5 | 1.7 | 1.9 | 2.1 | 2.3 | 2.5 |
| 9.375..... | ... | ... | ... | ... | ... | ... | ... | ... | ... | ... | 2 | ... | ... | ... | ... |
| 9.625..... | ... | ... | ... | ... | ... | ... | ... | ... | 2 | ... | 2 | ... | ... | ... | ... |
| 9.875..... | ... | ... | ... | ... | 1 | ... | 1 | ... | 2 | ... | ... | 1 | ... | ... | ... |
| 10.125..... | ... | ... | ... | ... | ... | 1 | 1 | 1 | 1 | 2 | ... | ... | ... | ... | 1 |
| 10.375..... | ... | ... | ... | ... | ... | 1 | 1 | ... | 1 | ... | ... | ... | ... | ... | ... |
| 10.625..... | ... | ... | ... | ... | ... | 1 | ... | ... | 2 | ... | ... | 1 | 2 | ... | ... |
| 10.875..... | ... | ... | ... | ... | ... | ... | ... | ... | ... | ... | ... | 2 | 1 | ... | ... |
| 11.125..... | ... | ... | ... | ... | 2 | ... | ... | 2 | ... | 2 | ... | 1 | 1 | ... | 1 |
| 11.375..... | ... | ... | ... | ... | ... | ... | ... | 2 | ... | ... | 4 | 2 | ... | ... | ... |
| 11.625..... | ... | ... | ... | ... | ... | ... | 1 | 3 | ... | 2 | 2 | 2 | ... | ... | ... |
| 11.875..... | ... | ... | ... | 2 | ... | ... | 2 | 3 | 2 | ... | 2 | 6 | ... | ... | ... |
| 12.125..... | ... | ... | ... | 1 | ... | 1 | 2 | ... | 1 | ... | 2 | 1 | ... | ... | ... |
| 12.375..... | ... | ... | ... | ... | 2 | ... | 1 | 4 | 2 | ... | 2 | ... | 1 | ... | ... |
| 12.625..... | ... | ... | 4 | 2 | 1 | 2 | 2 | 7 | 1 | ... | 3 | 1 | ... | 1 | 1 |
| 12.875..... | ... | ... | 1 | 1 | 3 | 1 | 4 | 3 | 4 | ... | 5 | ... | 1 | ... | ... |
| 13.125..... | ... | 2 | ... | 3 | 1 | 2 | 5 | 4 | 3 | 3 | 5 | ... | 1 | ... | ... |
| 13.375..... | ... | 3 | 1 | ... | ... | 1 | 8 | 5 | 4 | 2 | 5 | 2 | 1 | ... | 1 |
| 13.625..... | ... | ... | 6 | 1 | 1 | 4 | 11 | 6 | 4 | 3 | 3 | 3 | 2 | 1 | ... |
| 13.875..... | 1 | 4 | 2 | 5 | ... | 3 | 9 | 9 | 9 | 3 | 9 | ... | 1 | 3 | 1 |
| 14.125..... | 3 | 3 | 5 | 4 | 2 | 8 | 11 | 7 | 2 | 10 | 6 | 8 | 10 | 3 | 1 |
| 14.375..... | 6 | 5 | 7 | 3 | 5 | 3 | 11 | 12 | 11 | 19 | 5 | 18 | 24 | 7 | 2 |
| 14.625..... | 5 | 3 | 6 | 2 | 7 | 9 | 20 | 14 | 15 | 18 | 15 | 34 | 14 | 3 | 2 |
| 14.875..... | 11 | 6 | 7 | 6 | 4 | 12 | 21 | 23 | 34 | 26 | 42 | 11 | 4 | 1 | ... |
| 15.125..... | 11 | 18 | 8 | 8 | 7 | 12 | 18 | 16 | 42 | 81 | 59 | 7 | 1 | ... | 1 |
| 15.375..... | 18 | 14 | 13 | 7 | 14 | 18 | 34 | 41 | 66 | 174 | 20 | 3 | 1 | ... | ... |
| 15.625..... | 31 | 16 | 16 | 11 | 34 | 43 | 34 | 75 | 161 | 193 | 8 | ... | 5 | ... | ... |
| 15.875..... | 34 | 28 | 16 | 26 | 53 | 40 | 53 | 174 | 278 | 45 | 5 | 1 | ... | ... | ... |
| 16.125..... | 43 | 43 | 26 | 15 | 45 | 24 | 76 | 260 | 292 | 6 | 8 | 7 | 3 | ... | ... |
| 16.375..... | 53 | 53 | 26 | 25 | 34 | 28 | 148 | 370 | 162 | 9 | 5 | 4 | 3 | ... | ... |
| 16.625..... | 49 | 74 | 44 | 29 | 34 | 83 | 161 | 521 | 62 | 10 | 7 | 3 | ... | 1 | ... |
| 16.875..... | 38 | 118 | 52 | 21 | 29 | 119 | 303 | 633 | 75 | 7 | 8 | 4 | ... | ... | ... |
| 17.125..... | 54 | 139 | 89 | 31 | 67 | 210 | 529 | 741 | 226 | 22 | 6 | 2 | ... | ... | ... |
| 17.375..... | 55 | 191 | 348 | 392 | 115 | 322 | 874 | 1511 | 1441 | 320 | 26 | ... | ... | ... | ... |

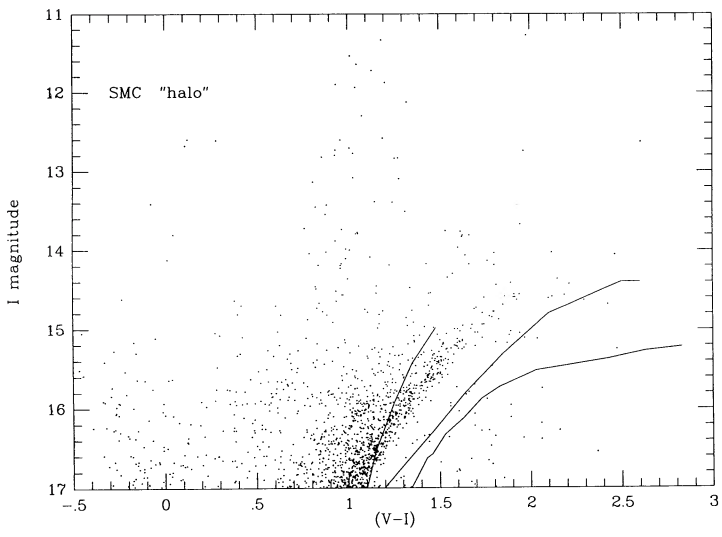


FIG. 1*a*

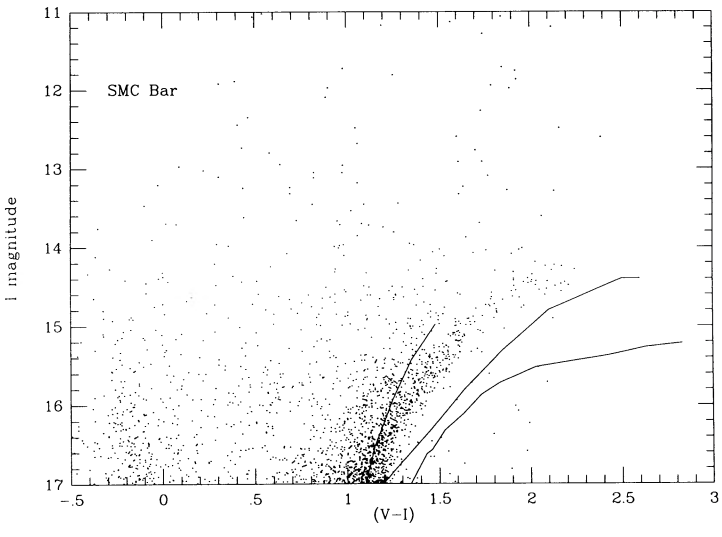


FIG. 1*b*

FIG. 1.—(*a*) The ($I$, $V-I$) color-magnitude diagram for a 0.2 deg$^2$ region of the SMC centered on $\alpha = 1^h8^m$, $\delta = 72°45'$, in the wing of the SMC. (*b*) The ($I$, $V-I$) color-magnitude diagram for the higher star density regions of our field, those sections nearer the bar of the SMC. The three giant branches plotted are schematic representations of, from blue to red, M92, field stars in the LMC, and 47 Tucanae.

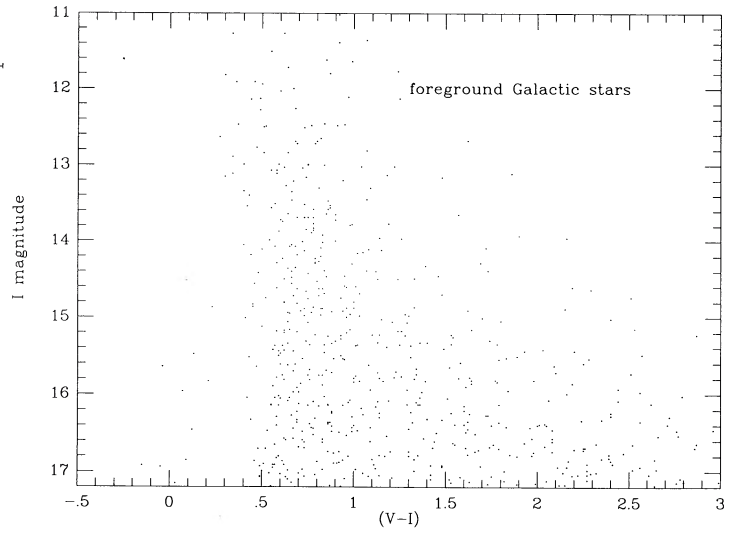


FIG. 2.—The color-magnitude diagram for foreground Galactic stars as predicted by the star-count model discussed in § II.

magnitude diagram, an $r^{-3.5}$ density law, axial ratio $b/a = 0.6$, and a local number density of 0.002 of the disk.

Figure 2 shows the color-magnitude diagram that the model predicts for foreground stars in the SMC field. Lying at $l = 300°$, $b = -48°$, a significantly higher latitude than the LMC, only $\sim 560$ Galactic stars with $I \leq 17.0$ are predicted, as compared with the 9247 stars that are observed. Thus the form of the corrected color-magnitude diagram is not sensitive to the parameters adopted in the Galactic model. Using the star catalog generated by the model, we have cleaned the observed color-magnitude diagram, removing stars that lie within a certain tolerance ($\pm 0.15$ mag) of individual "stars" in the model. The resulting color-magnitude diagram is shown in Figure 3.

The morphology of the red giant branch has long been used as an abundance estimator and, with due allowance for the uncertainties in calibration, we can apply our data to this end.

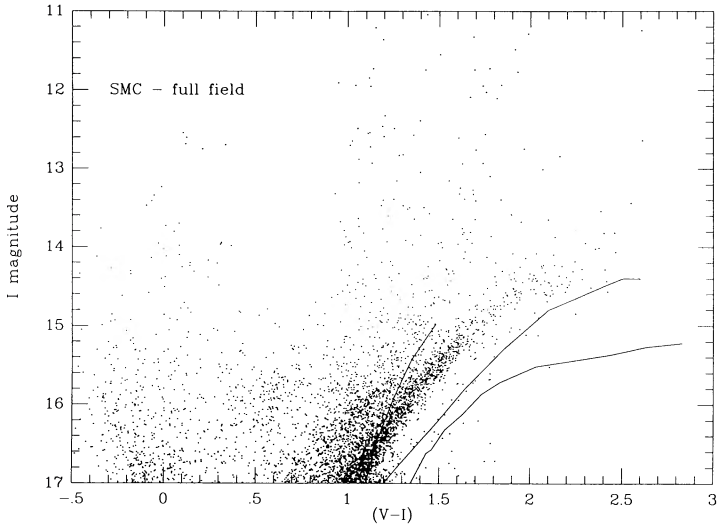


FIG. 3.—The ($I$, $V-I$) color-magnitude diagram for the complete 0.57 deg$^2$ field covered by our survey. We have allowed for contamination by foreground Galactic stars.

There are relatively few abundance estimates for the older stellar population in the SMC, and those derived from individual stars are concentrated within the outlying NGC 121 field studied by Graham (1975). Suntzeff *et al.* (1986) find a mean abundance of [M/H] $= -1.6 \pm 0.3$ for 30 red giants in this field, while Butler, Demarque, and Smith (1982) have determined a mean abundance of $\langle$[Fe/H]$\rangle = -1.8$ from several RR Lyraes and $\langle$[Fe/H]$\rangle = -1.3$ from three "overluminous" variables. They infer an age of 6–7 Gyr for the latter stars. Color-magnitude diagram studies of intermediate-age and old SMC clusters give abundance estimates of from [Fe/H] $= -0.9 \pm 0.3$ for NGC 411 (Da Costa and Mould 1986), relatively close to the bar, to [Fe/H] $= -1.4 \pm 0.3$ for the outlying cluster Lindsay 113 (Mould, Da Costa, and Crawford 1984).

Considering our observations, Figures 1 and 3 also include schematic representations of the giant branch sequences in M92, 47 Tuc, and in the LMC Shapley III field (from RMT87). The SMC giant branch is substantially bluer than the latter two sequences, lying close to the metal-poor M92 giant branch, although with a slope that is more similar to that of the giant branch of the LMC and of the metal-rich cluster 47 Tuc. We have already commented on the uncertainty of the color corrections, and these could affect either the shape or the position (in $V-I$) of the giant branch. However, both LMC and SMC data are based on the same photographic material calibrated using the same methods; thus the difference in color between the two is better established, with the SMC field stars clearly more metal-poor.

Mould, Kristian, and Da Costa (1983) have shown that one can use the mean $V-I$ color at $M_I = -3$ to estimate the mean metallicity of a stellar population. Da Costa and Armandroff (1990) have mapped the giant branch in the ($M_I$, [$V-I$]) plane for six galactic globulars, spanning the abundance range $-2.2 \leq$ [Fe/H] $\leq -0.7$. Their data show that the giant branch steepens noticeably with decreasing abundance. Taking the SMC color distribution at $M_I = -3.0 \pm 0.25$ ($15.63 \leq I \leq 16.13$, for $[m - M] = 18.8$, $A_I = 0.08$), the mean $(V-I)_0$ is $\sim 1.25$ mag, comparable with that of the NGC 6752 giant branch at the same luminosity and implying [M/H] $\sim -1.5$. As a measure of the uncertainty, if we assume we have underestimated $V-I$ by 0.15 mag, the implied abundance is [M/H] $\sim -1.2$ (and the revised calibration for the Shapley III LMC data implies [M/H] $\sim -0.7$), while moving the giant branch to the blue gives [M/H] $\sim -2$ ($\sim -1.5$ for the LMC). Differences in age between the Magellanic populations and the clusters may also lead to our underestimating the abundance. Given that the region surveyed here lies near the main body of the SMC, one might expect a higher mean abundance than in outlying fields, something also suggested by the shape of the giant branch. Comparing the two color-magnitude diagrams in Figure 1, the giant branch appears to extend slightly further to the red in the bar field. It is possible that this reflects a larger range in abundance within the bar of the SMC than in the outer halo region, although the effect could also arise from higher photometric uncertainties in the regions of higher star density.

### c) *The Asymptotic Giant Branch Population*

It is clear that, even after subtraction of the foreground Galactic stars, there remain a moderate number of stars occupying positions above the SMC giant branch. These include both intermediate-age asymptotic giant branch stars and their Cepheid progenitors, and more recently formed stars which

have evolved beyond the main-sequence turnoff. In particular, the clump of red stars at $I \sim 12$, $V-I \sim 1.6$ are most likely to be young supergiants. There is also a relatively small, but significant, number of stars lying up to 1 mag above the clearly defined SMC giant branch. Most of these are probably young and intermediate-age giants, the product of continuing star formation in the SMC. However, there is some evidence suggesting that the SMC has a significant depth, up to 20 kpc, along the line of sight (Mathewson, Ford, and Visvanathan 1988), and it is possible that some are giants lying within a foreground region of the SMC. We shall discuss this point in greater detail in § V.

Turning to the asymptotic giant branch, as in our previous studies of the LMC, we have used the data in our photometric catalog to calculate an AGB luminosity function. The color-magnitude diagram indicates that the bulk of the stars are comparable in metal abundance to the metal-poor Galactic globular clusters. Hence we have included all stars with $(V-I)_0 > 1.50$ ($V-I > 1.55$) as AGB candidates; that is, we include all stars redder than the color of the tip of the M92 giant branch. Bolometric corrections have been calculated using Bessell and Wood's (1984) formula

$$\mathrm{BC}_I = 0.3 + 0.38 \times (V-I)_0 - 0.14 \times (V-I)_0^2 .$$

This is appropriate for M and S stars (except for the very latest spectral types), which constitute the bulk of our sample. However, if we apply the C-star formula used by Reid and Mould (1985),

$$\mathrm{BC}_I = 1.9 - 0.7 \times (V-I)_0 ,$$

the differences in computed $M_{\mathrm{bol}}$ range from only +0.33 (in the sense that the C-star formula gives a larger bolometric correction) at $(V-I)_0 = 1.45$ to $-0.20$ at $(V-I)_0 = 2.45$. The absolute bolometric magnitude then follows from

$$M_{\mathrm{bol}} = I + \mathrm{BC}_I - 18.8 - A_I ,$$

where $A_I = 0.08$ mag. Note that an uncertainty of 0.15 mag in $V-I$ affects $\mathrm{BC}_I$ by less than 0.1 mag for $V-I \leq 1.5$—the color range most subject to uncertainty, as discussed in § II*a*.

We have been able to check the completeness of our sample, at least for carbon stars, against the results obtained by Blanco and McCarthy using objective prism techniques. Their data cover 28 fields in the SMC (Blanco and McCarthy 1983), each 0.12 deg$^2$ in area. One of these fields, no. 23, centered on NGC 416, falls almost completely within the area covered by our survey, and V. M. Blanco kindly has made available the plate of this field. Of the 24 carbon stars identified, one lies beyond the southern limit of our plate material, and four are merged images on the COSMOS scans. All the remaining stars have $V-I$ colors of at least $V-I = 1.6$; most have $V-I > 2$, and all are included in our AGB sample. This implies a completeness of more than 80%, and it is likely that the same factor applies to M-type AGB stars.

## III. SPECTROSCOPIC OBSERVATIONS

In order to refine the accuracy of our determination of the AGB star luminosity function, we have obtained spectroscopic observations of selected subsamples of the candidate AGB stars. In particular, our previous studies of stars in the LMC revealed many early-type (K3–K5) red giants amongst the more luminous stars which exhibit none of the abundance characteristics that one associates with dredge-up in double-shell-burning stars. We have suggested that a significant fraction of these stars could be massive ($>10\ M_\odot$) stars on their first ascent of the giant branch. Given the presence of greater than 15 $M_\odot$ main-sequence stars in the field currently under study, it is likely that such stars make some contribution to our sample of AGB candidates.

We have obtained observations of four subsamples drawn from the AGB candidates. First, covering the full 0.82 deg$^2$ field, we have observed 42 of the 47 stars with $M_{\mathrm{bol}} \leq -5.50$ and $(V-I)_0 \geq 1.55$. Data for these stars, together with a number of redder, lower luminosity stars (C-star candidates), are given in Table 3. Second, we chose three smaller areas, each of solid angle 80 arcmin$^2$, and we have taken spectra of most AGB candidates with $M_{\mathrm{bol}} \leq -3.25$ in each of these fields. These observations are listed in Table 4. The three fields cover a range of environments, with fields 2 and 3 near the bar, while field 1 is in the "halo" region. Finally, we also have observed other AGB candidates with $M_{\mathrm{bol}} \leq -5.0$ and $(V-I)_0 \geq 2.0$, and these stars are listed in Table 3.

Our spectroscopic observations were obtained using the modular spectrograph on the 2.5 m du Pont telescope at Las Campanas observatory. This spectrograph, described in detail by Schechter (1988), can be used in several modes. Our data were taken using a cross-dispersed echellette configuration, with a 100 lines mm$^{-1}$ reflection grating and 200 lines mm$^{-1}$ transmission grating as cross-disperser. The spectra cover the wavelength range ~4700 Å to ~9600 Å in ten orders, although the system response is low for $\lambda \leq 5000$ Å. The detector is an 800 × 800 format TI chip with 15 $\mu$ pixels, and the dispersion given by the system is ~70 km s$^{-1}$ per pixel, while the resolution varies from 1.7–2.5 pixels (FWHM) across the chip.

The observations were obtained during the period 1988 October 23/24 to October 30/31, with conditions photometric and seeing ~1″.0 to 1″.5 on each night. The slit width was set to 1″.5 throughout the run, giving a projected slit width of 1.8 pixels at the detector. Wavelength calibration was defined using exposures of helium, neon, and argon lamps. With our observations restricted to a small region within the SMC, these calibration exposures were taken after every third program star. Cross-correlating arc spectra taken during the run, the largest drift in wavelength scale between successive calibration exposures is only 0.2 pixels, or 13 km s$^{-1}$.

Our data reduction methods are presented and discussed in Reid, Tinney, and Mould (RTM90). To summarize, the curved echelle orders were straightened, extracted with the appropriate sky subtraction, wavelength calibrated, and set on a flux scale using observations of LTT 9239 (Stone and Baldwin 1983). Adjacent orders overlap, allowing the data to be merged to give a continuous one-dimensional spectrum, and a comparison with other flux standards indicates that the final flux calibration is accurate to $\sim \pm 10\%$. We also have attempted to compensate for the terrestial atmospheric absorption features in the near-infrared ($\lambda > 7000$ Å) by dividing the spectra by a normalized spectrum of the early-type star Hiltner 600; we have used a continuum-fitting routine to remove the H-Paschen lines in the latter's spectrum. The terrestial features, which are primarily caused by OH, show significant variations, both temporal and as a function of air mass, and the process was rarely completely successful.

We have determined radial velocities for the program stars by cross-correlation against the Galactic stars HD 189711 (C star), Vyssotsky 5 (M5S), and HR 7176 (K giant). As indicated

TABLE 3

LUMINOUS AGB STAR CANDIDATES

| $n$ | $\alpha$ | $\delta$ | $I$ | $V-I$ | $M_{bol}$ | Spectral Type | $V_r$ |
|---|---|---|---|---|---|---|---|
| B4 | $1^h13^m42^s.7$ | −72°51′49″ | 13.81 | 2.34 | −4.57 | C | 163 |
| B99 | 1 09 08.7 | −72 31 59 | 14.01 | 2.32 | −4.60 | C | 162 |
| B219 | 1 06 31.9 | −72 34 03 | 13.77 | 2.19 | −4.65 | M3 | 144 |
| B58 | 1 10 39.8 | −73 08 16 | 13.81 | 2.40 | −4.82 | C | 207 |
| B213 | 1 06 35.9 | −73 01 30 | 13.54 | 2.33 | −5.04 | C | 165 |
| B162 | 1 07 35.6 | −72 30 50 | 13.43 | 2.49 | −5.26 | C | 186 |
| B265 | 1 05 34.7 | −73 00 07 | 13.29 | 2.08 | −5.11 | K5 | 190 |
| B128 | 1 08 12.2 | −72 58 18 | 12.84 | 2.11 | −5.56 | M3 | 201 |
| B229 | 1 06 21.8 | −72 59 27 | 12.76 | 1.65 | −5.57 | K5 | 191 |
| B28 | 1 12 12.8 | −73 00 38 | 12.74 | 1.91 | ... | M2 V | 5 |
| B230 | 1 06 24.8 | −72 56 25 | 12.60 | 1.55 | −5.73 | ... | ... |
| B155 | 1 07 44.0 | −72 32 31 | 12.56 | 1.70 | −5.78 | K5 | 169 |
| B293 | 1 04 59.5 | −72 31 04 | 12.52 | 1.73 | −5.67 | C | 194 |
| B146 | 1 07 53.8 | −72 31 35 | 12.46 | 1.65 | −5.88 | K5 | 196 |
| B357 | 1 03 32.3 | −73 05 42 | 12.60 | 2.34 | −5.85 | M4S | 188 |
| B84 | 1 09 36.4 | −72 43 32 | 12.63 | 2.55 | ... | M5 V | 105 |
| B332 | 1 04 04.4 | −73 07 10 | 12.49 | 2.11 | ... | M4 V | 7 |
| B335 | 1 04 06.6 | −72 37 28 | 12.27 | 1.68 | −6.07 | K4 | 190 |
| B240 | 1 06 08.1 | −72 32 30 | 12.10 | 1.76 | −6.24 | K5 | 133 |
| B29 | 1 12 12.0 | −73 11 09 | 12.08 | 1.61 | −6.26 | ... | ... |
| B183 | 1 07 22.2 | −72 24 21 | 12.02 | 1.77 | −6.33 | K5 | 138 |
| B271 | 1 05 30.1 | −72 51 36 | 11.98 | 1.84 | −6.37 | K5 | 208 |
| B104 | 1 09 01.4 | −73 05 32 | 11.94 | 1.68 | −6.40 | K5 | 134 |
| B264 | 1 05 40.7 | −72 44 35 | 11.94 | 1.74 | −6.40 | ... | ... |
| B115 | 1 08 43.3 | −72 53 29 | 11.93 | 1.78 | −6.42 | K5 | 176 |
| B362 | 1 03 35.1 | −72 32 49 | 11.89 | 1.80 | ... | M2 V | 10 |
| B327 | 1 04 08.1 | −73 04 45 | 11.86 | 1.88 | −6.50 | K5 | 188 |
| B294 | 1 04 58.6 | −72 33 22 | 11.83 | 1.79 | −6.52 | K5 | 133 |
| B24 | 1 12 29.4 | −73 07 34 | 11.74 | 1.64 | −6.59 | K4 | 141 |
| B238 | 1 06 04.3 | −72 55 15 | 11.76 | 1.87 | −6.60 | K5 | 185 |
| B139 | 1 08 01.6 | −72 29 40 | 11.72 | 1.72 | −6.62 | M0 | 188 |
| B350 | 1 03 43.9 | −72 55 32 | 11.71 | 1.80 | −6.64 | K5 | 162 |
| B348 | 1 03 52.5 | −72 33 08 | 11.53 | 1.87 | −6.83 | K5 | 156 |
| B148 | 1 07 48.4 | −73 01 41 | 11.48 | 1.86 | −6.87 | K5 | 150 |
| B376 | 1 03 20.5 | −72 31 11 | 11.46 | 1.72 | −6.88 | K5 | 154 |
| B333 | 1 04 15.4 | −72 28 39 | 11.38 | 1.72 | ... | M0 V | 54 |
| B88 | 1 09 30.7 | −73 04 32 | 11.32 | 1.63 | ... | K5 III | 40 |
| B317 | 1 04 27.9 | −72 40 07 | 11.28 | 1.69 | −7.06 | K5 | 163 |
| B91 | 1 09 24.2 | −72 41 37 | 11.28 | 1.93 | −7.09 | K5 | 196 |
| B340 | 1 03 55.7 | −72 56 26 | 11.13 | 1.58 | −7.20 | K5 | 163 |
| B306 | 1 04 31.0 | −73 08 21 | 11.20 | 2.07 | −7.20 | K5 | 186 |
| B120 | 1 08 34.5 | −72 52 51 | 11.24 | 2.55 | −7.28 | M6 | 210 |
| B284 | 1 05 07.3 | −72 44 48 | 11.06 | 1.79 | −7.29 | K5 | 156 |
| B363 | 1 03 19.3 | −73 03 55 | 10.83 | 1.85 | −7.52 | ... | ... |
| B244 | 1 06 07.4 | −72 42 47 | 10.85 | 2.03 | −7.53 | K5 | 151 |
| B248 | 1 05 57.5 | −72 46 47 | 10.80 | 1.92 | −7.57 | K5 | 150 |
| B307 | 1 04 29.1 | −73 08 48 | 10.71 | 2.02 | −7.68 | K4 | 198 |
| B231 | 1 06 16.7 | −72 39 44 | 10.68 | 2.02 | −7.70 | K5 | 142 |
| B174 | 1 07 20.8 | −72 39 07 | 10.52 | 1.92 | −7.85 | K5 | 165 |
| B124 | 1 08 26.9 | −72 36 42 | 10.14 | 1.55 | ... | K4 III | −3 |
| B154 | 1 07 43.6 | −72 28 48 | 10.22 | 2.40 | ... | M4 V | −1 |
| B96 | 1 09 24.9 | −72 51 16 | 9.96 | 1.92 | −8.42 | ... | ... |
| B270 | 1 05 35.8 | −72 46 48 | 9.66 | 1.56 | ... | K4 III | 21 |
| B374 | 11 03 23.0 | −72 24 52 | 9.57 | 1.87 | ... | M0 III | 8 |

in RTM89, a comparison of our results with catalog velocities gives an rms accuracy of 19 km $s^{-1}$ (21 stars). The radial velocities of the SMC stars are listed with the positions and photometry in Table 4, where we also present our own observations of stars of known radial velocity and spectral type.

## IV. THE SPECTRAL CHARACTERISTICS OF SMC AGB STARS

### *a) The Luminous Red Giants: AGB Stars or Supergiants*

The observations described in § III allow us to refine the photometrically defined AGB luminosity function both by using a series of narrow-band spectroscopic indices to identify non–AGB stars, and by using the radial velocities to identify foreground Galactic stars. Foreground dwarfs can be eliminated since they have substantially stronger Na D lines than are found in lower gravity giants of the same temperature, while Galactic giants can be identified from the radial velocity measurements, although there is some ambiguity in the latter process. The SMC has more complex kinematics than the larger LMC, with known members exhibiting radial velocities of from ~120 to ~200 km $s^{-1}$. Stars within the Galactic halo can also have velocities within this range, although relatively few (1–2) are expected within our 0.82 $deg^2$ field. The Galactic

TABLE 4

AGB STARS IN SELECTED REGIONS

| $n$ | $\alpha$ | $\delta$ | $I$ | $V-I$ | $M_{bol}$ | Spectral Type | $V_r$ |
|---|---|---|---|---|---|---|---|
| Field 1: $\alpha = 1^h8^m.6$, $\delta = -72°58'$ | | | | | | | |
| 1..... | $1^h09^m03^s.2$ | −73°01′56″ | 15.33 | 1.64 | −3.00 | ... | ... |
| 2..... | 1 08 16.4 | −73 00 29 | 15.26 | 1.61 | −3.07 | M0 | 103 |
| 3..... | 1 08 10.7 | −72 56 41 | 15.10 | 1.63 | −3.23 | K3 | 142 |
| 4..... | 1 08 12.2 | −72 58 18 | 12.84 | 2.11 | −5.56 | M3 | 201 |
| 5..... | 1 08 12.3 | −73 00 09 | 14.44 | 1.90 | −3.92 | M0 | 169 |
| 6..... | 1 08 00.1 | −72 57 33 | 14.49 | 1.76 | −3.85 | M0 | 110 |
| 7..... | 1 07 48.4 | −73 01 41 | 11.48 | 1.86 | −6.87 | M0/1 | 156 |
| Field 2: $\alpha = 1^h4^m.15$, $\delta = -73°2'$ | | | | | | | |
| 1..... | 1 04 51.3 | −73 02 17 | 14.19 | 1.98 | −4.14 | C | 159 |
| 2..... | 1 04 43.1 | −72 56 23 | 13.69 | 1.67 | −4.65 | K5 | 146 |
| 3..... | 1 04 37.0 | −72 57 56 | 14.03 | 1.89 | ... | K4 III | 23 |
| 4..... | 1 04 32.8 | −73 00 59 | 15.06 | 1.56 | −3.26 | ... | ... |
| 5..... | 1 04 22.1 | −73 02 14 | 15.14 | 1.58 | −3.19 | ... | ... |
| 6..... | 1 04 18.5 | −72 55 30 | 14.81 | 1.77 | ... | M3 V | 228 |
| 7..... | 1 04 16.1 | −72 57 06 | 14.48 | 1.98 | −3.85 | C | 196 |
| 8..... | 1 04 12.0 | −72 58 51 | 14.58 | 1.55 | −3.46 | K4 | 199 |
| 9..... | 1 04 09.0 | −72 59 33 | 14.99 | 1.62 | −3.35 | M0 | 111 |
| 10..... | 1 03 58.8 | −73 01 53 | 12.91 | 1.56 | −5.41 | ... | ... |
| 11..... | 1 03 55.7 | −72 56 26 | 11.13 | 1.58 | −7.20 | K5 | 163 |
| 12..... | 1 03 53.7 | −72 55 40 | 14.44 | 1.96 | −3.90 | C | 210 |
| 13..... | 1 03 52.6 | −72 55 41 | 14.79 | 1.76 | −3.55 | M2 | 195 |
| 14..... | 1 03 53.4 | −73 00 19 | 14.73 | 1.72 | −3.45 | C | 152 |
| 15..... | 1 03 43.9 | −72 55 32 | 11.71 | 1.80 | −6.64 | K5 | 162 |
| 16..... | 1 03 46.4 | −72 55 42 | 14.74 | 1.92 | −3.62 | C | 160 |
| 17..... | 1 03 42.7 | −73 01 01 | 14.91 | 1.61 | −3.43 | K4 | 197 |
| 18..... | 1 03 40.1 | −72 58 17 | 14.01 | 1.91 | ... | M3 V | −9 |
| 19..... | 1 03 24.0 | −72 59 17 | 14.35 | 1.74 | −3.92 | C | 1900 |
| 20..... | 1 03 15.4 | −72 53 12 | 14.49 | 1.92 | −3.80 | C | 150 |
| Field 3: $\alpha = 1^h4^m.3$, $\delta = -72°35'$ | | | | | | | |
| 1..... | 1 04 59.5 | −72 31 04 | 12.52 | 1.73 | −5.67 | C | 194 |
| 2..... | 1 04 58.6 | −72 33 22 | 11.83 | 1.79 | −6.52 | K5 | 133 |
| 3..... | 1 04 39.1 | −72 31 48 | 15.12 | 1.63 | −3.21 | M0 | 178 |
| 4..... | 1 04 41.0 | −72 32 56 | 14.31 | 2.21 | −4.18 | C | 149 |
| 5..... | 1 04 34.3 | −72 38 03 | 15.26 | 1.56 | −3.07 | ... | ... |
| 6..... | 1 04 29.1 | −72 33 35 | 14.75 | 1.82 | −3.48 | C | 121 |
| 7..... | 1 04 18.5 | −72 35 06 | 14.56 | 2.12 | −3.87 | C | 187 |
| 8..... | 1 04 19.1 | −72 37 26 | 14.45 | 2.14 | ... | M4 III | 73 |
| 9..... | 1 04 16.1 | −72 32 43 | 13.67 | 1.61 | −4.66 | ... | ... |
| 10..... | 1 04 08.6 | −72 29 43 | 14.43 | 1.98 | −3.90 | C | 196 |
| 11..... | 1 04 06.6 | −72 37 28 | 12.27 | 1.68 | −6.07 | K5 | 190 |
| 12..... | 1 03 58.5 | −72 30 53 | 15.30 | 1.75 | −3.05 | ... | ... |
| 13..... | 1 03 52.5 | −72 33 08 | 11.53 | 1.87 | −6.83 | K5 | 156 |
| 14..... | 1 03 51.9 | −72 36 11 | 14.07 | 1.64 | −4.26 | M0 | 197 |
| 15..... | 1 03 42.4 | −72 33 39 | 14.51 | 1.83 | −3.85 | M1 | 136 |
| 16..... | 1 03 35.1 | −72 32 49 | 11.89 | 1.80 | ... | M2 V | 10 |
| 17..... | 1 03 24.1 | −72 30 32 | 14.16 | 2.00 | −4.22 | M4 | 136 |
| 18..... | 1 03 23.8 | −72 33 53 | 15.04 | 1.64 | −3.30 | K5 | 120 |

NOTE.—The following stars are also listed in Table 3: SMC 1-4 = B128; SMC 2-11 = B340; SMC 3-1 = B293; SMC 3-2 = B294; SMC 3-11 = B335; SMC 3-13 = B348; and SMC 3-16 = B362.

stars, both dwarfs and giants, are identified (by the suffixes V and III, respectively) in Tables 3 and 4.

Considering the remaining stars, two important points should be made. First, the vast majority of luminous AGB candidates ($M_{bol} < -6$) are of type K4 or K5 and show little or no evidence for TiO bands in the spectrum (as measured by the indices centered on the 6260 and 7060 band heads); second, while the most luminous C stars in the field are at $M_{bol} = -5.7$ (SMC B293), there is evidence for S-type features in the later type, more luminous SMC B357.

Of the 28 SMC stars with $M_{bol} < -5.5$, only four are cool enough to show TiO absorption and, in one of these four cases, SMC B139, the evidence for molecular features is marginal. Figure 4*a* plots the spectrum of this star, which shows a suggestion of a weak depression near to 6260 (and perhaps 7060) TiO band head. Of the other three stars, SMC B357 (Fig. 4*c*) has strong TiO (spectral type ~ M3) as well as a moderately strong $\lambda$6475 ZrO (0, 0) band head. ZrO also has strong band heads at $\lambda$9350 (Bessell 1985), which are particularly prominent in late-type MS and S stars (see our spectrum of Vyssotsky 5, Fig. 4*b*). Terrestial $H_2O$ absorption is also present at these wavelengths, and Figure 4*c* shows this region of the spectrum in SMC B357

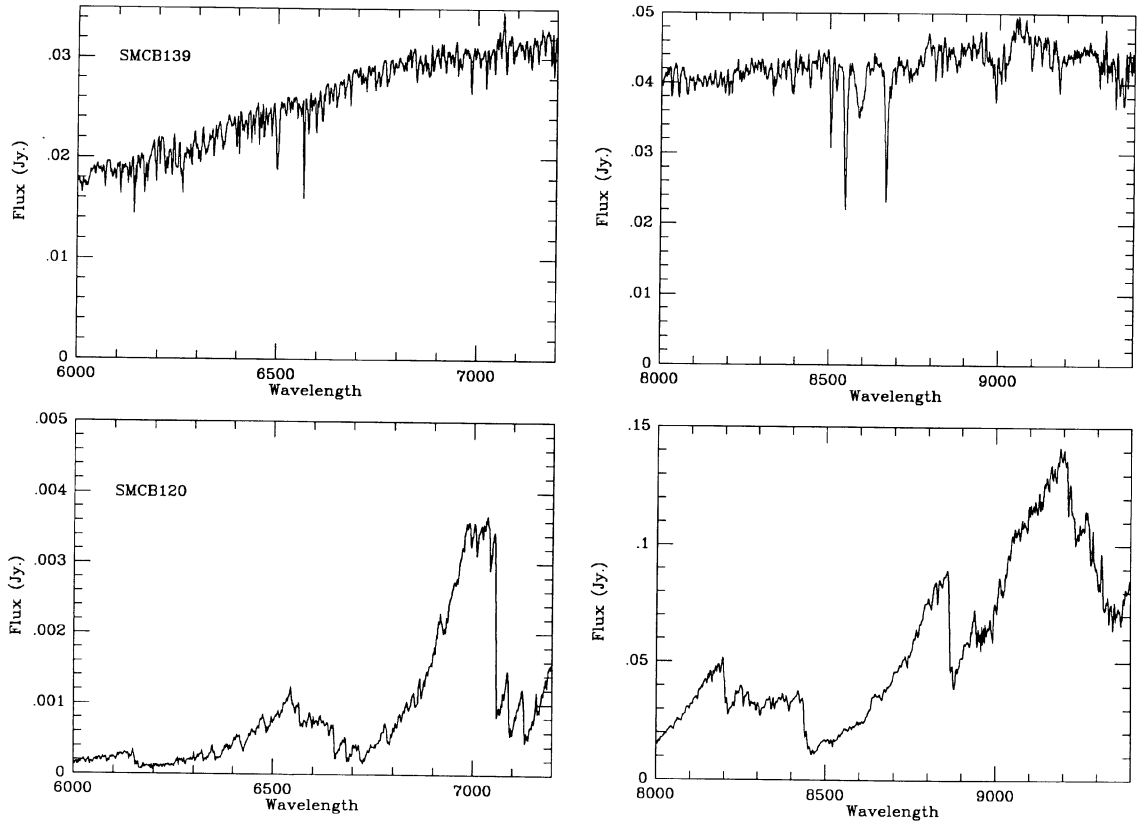


FIG. 4*a*

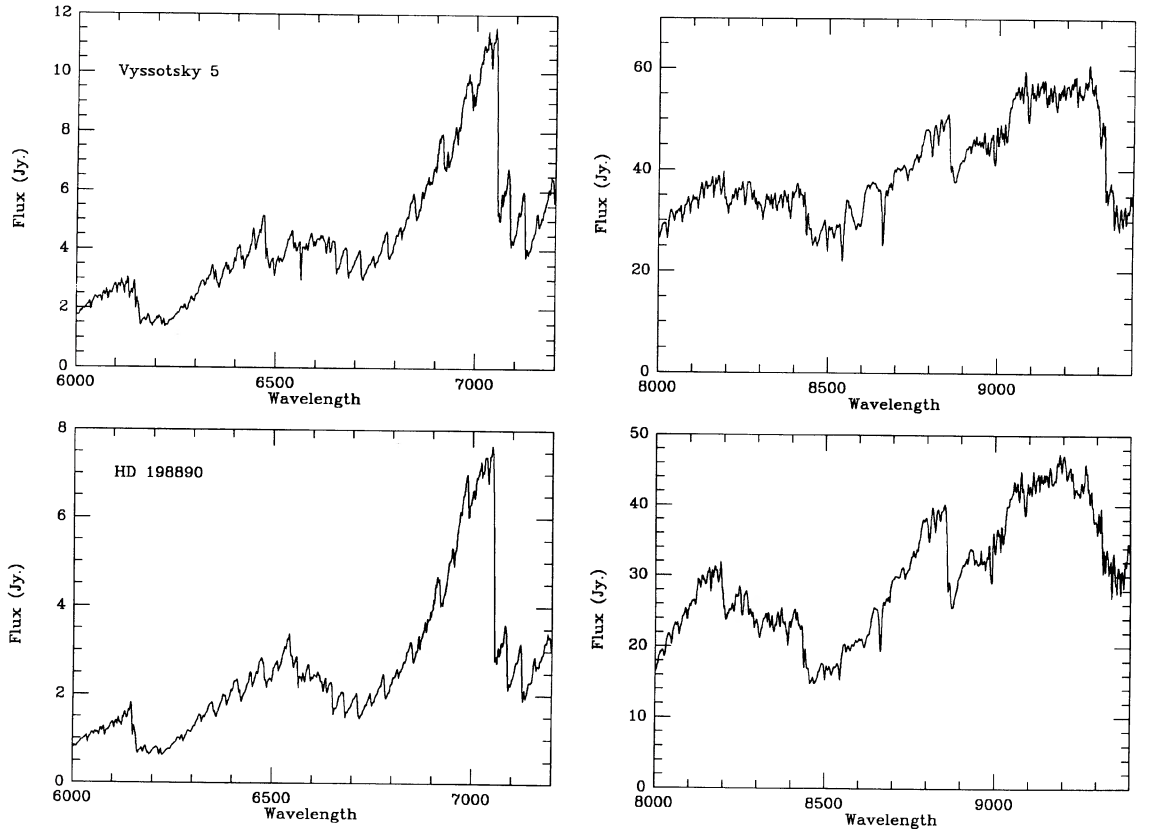


FIG. 4*b*

FIG. 4.—(*a*) Two of the most luminous SMC AGB stars: SMC B139, which may have weak TiO absorption, and SMC B120, the long-period variable HV 2112. The broad feature at 8600 Å which is evident in the former spectrum is an artifact introduced by a dead column in the CCD. (*b*) Spectra of the Galactic S star Vyssotsky 5 and of the star HD 198890, classified as M6, but exhibiting moderate strength ZrO bands at 6475 and 9400 Å. (*c*) Spectra of the remaining two AGB stars with $M_{bol} < -6$ which are cool enough to show TiO absorption: SMC B357 and SMC B128. (*d*) Spectra of SMC B115, one of the two luminous AGB candidates which has emission at Hα, and SMC B293, the highest luminosity C star in our sample.

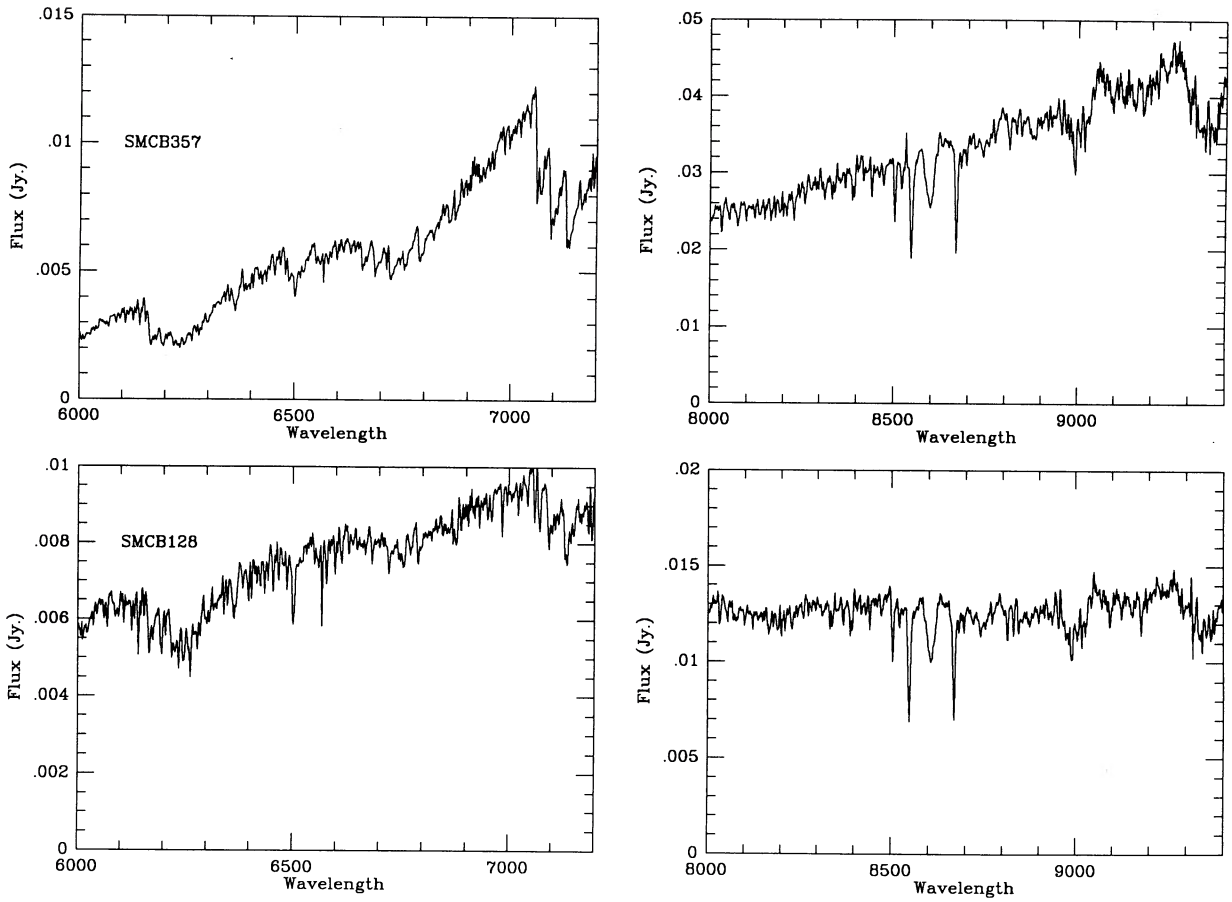


FIG. 4*c*

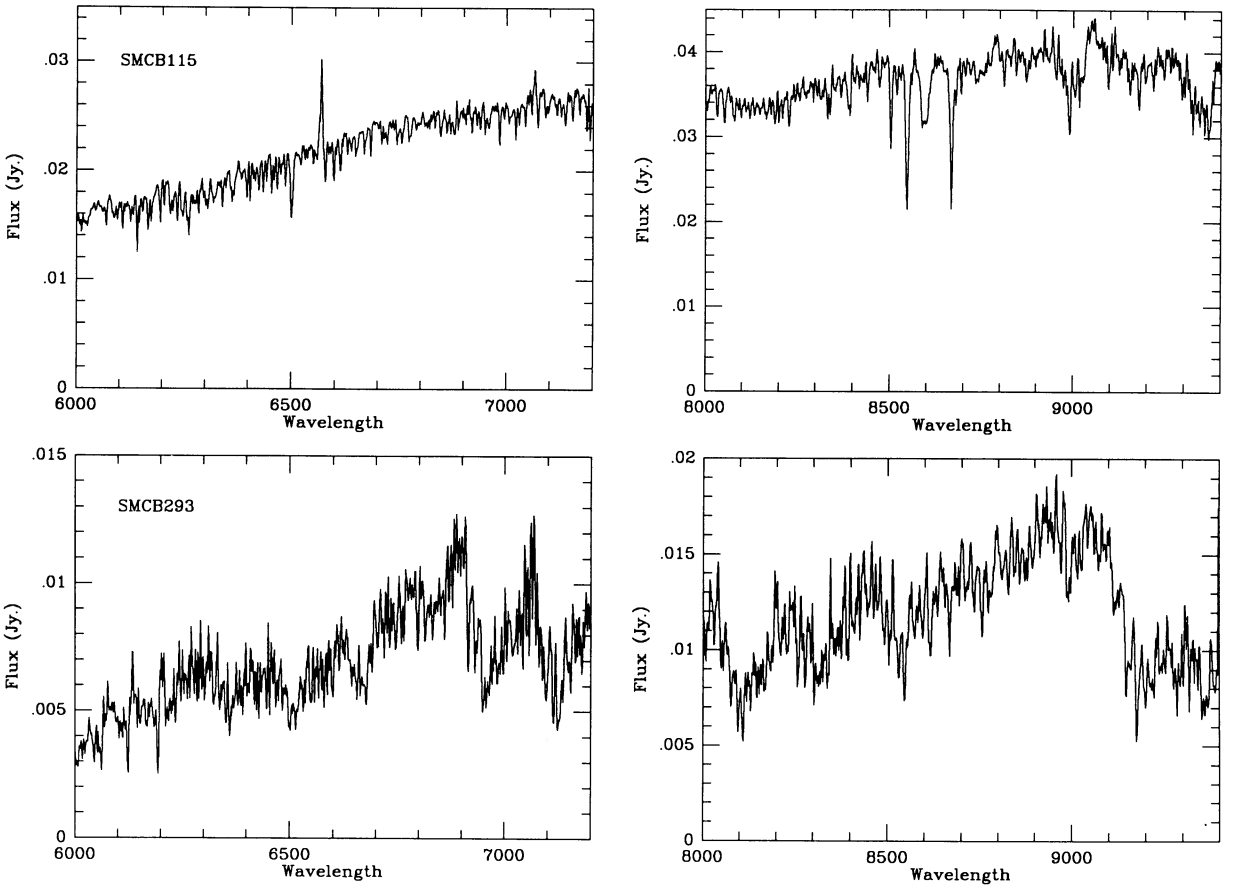


FIG. 4*d*

after division by the normalized spectrum of Hiltner 600. It is clear that, while not as prominent as in the cooler Vyssotsky 5, ZrO is present in the spectrum. However, with the uncertainties in subtracting the atmospheric features, the $\lambda$6475 band is as effective an S-star discriminant as the stronger infrared feature. In passing, we comment that the Galactic giant HD 198890, classified as M6 in the Michigan spectral catalog, also appears to have moderately strong ZrO and should be reclassified as M6S (Fig. 4*b*).

Both the remaining late-type stars, however appear to be M-type giants. The brighter of the two, SMC B120, is the variable star HV 2112 (Fig. 4*a*). With a period of 608 days and a bolometric magnitude of $m_{bol} \sim 11.9$ ($M_{bol} = -6.9$) (Wood, Bessell, and Fox 1983, hereafter WBF), this star lies at the upper end of the luminosity range of AGB stars. However, there is no evidence for S-star characteristics in the spectrum. WBF give spectral types of M3 to M7.5 from their observations, and we estimate a type of M6 from our spectrum. The final later type giant amongst the luminous SMC sample is of higher temperature, SMC B128, (Fig. 4*c*), spectral type M2, and $M_{bol} = -5.5$. Again there is no evidence for either ZrO absorption or enhanced Ba II lines in the spectrum. These two giants, then, are similar to the LMC stars LMC 423 (Reid and Mould 1985) and HV 2578 (WBF), stars which have evolved close to the tip of the AGB without having undergone sufficient dredge-up to change their surface composition.

Smith and Lambert (1989) recently obtained observations of five luminous ($M_{bol} = -6$ to $-7$) AGB stars in the SMC and found Li to be overabundant in all five stars. Our observations include one of these stars, HV 1963, and, despite the substantially lower resolution of our data ($\lambda/\Delta\lambda \sim 2000$, rather than 20,000), the strong Li I 6707.8 doublet is clearly visible (Fig. 5*a*). However, neither HV 2112 nor SMC B128 show evidence for a similar enhancement, although the fainter S-star SMC B357 does. We also were able to obtain observations of a number of LMC long-period variables (from Reid, Glass, and Catchpole 1988) during this same observing run, and three of these stars (V69, V7, and V15) appear to have strong Li 6707.8 (Fig. 5*b*). All three are brighter than $M_{bol} = -6$, and both V7 and V15 have moderate strength ZrO $\lambda$6473, although V69 does not appear to exhibit ZrO. Thus enhanced Li appears to be a relatively common phenomenon in the LMC.

Our observations show that 22 of the remaining 25 SMC red giants with $-5.5 \geq M_{bol} \geq -7.3$ are of spectral type K4 or K5, and the three stars for which we have no spectroscopic data are all bluer than $V-I = 1.8$, suggesting that these last are spectroscopically similar. Two of these earlier type stars, SMC B294 and SMC B115, have strong H$\alpha$ emission, and the spectrum of the latter star is plotted in Figure 4*d*. Figure 6*a* shows the distribution of spectral types as a function of luminosity for the luminous AGB sample.

Matching our derived luminosity function for all photometrically defined AGB stars against a continuous star formation model, it is evident that there is a significant excess of stars more luminous than $M_{bol} \sim -5.5$ as compared with the model (Fig. 6*b*). Indeed, even a model with a star formation rate increased by a factor of 20 for the last $10^8$ yr fails to predict the number of bright red giants that are observed. However, in this model we have computed only the AGB population; that is, no account is taken of the massive (10 $M_\odot$ or more) supergiants that would have been produced in recent (few $\times$ $10^6$ yr old) bursts of star formation. In our studies of the LMC, we have suggested that many of the bright, earlier type red giants found in that galaxy are young, core helium–burning supergiants (Mould and Reid 1987). There is a young population in this field (see the blue main sequence); is the number of "supergiants" consistent with the number of evolved stars expected from that population?

Mermilliod and Maeder (1986) have constructed composite color-magnitude diagrams by combining observations of Galactic open clusters of similar age. While the data are still sparse, it is possible to get an estimate of the expected relative numbers of red supergiants and luminous main-sequence stars. Thus, in the NGC 3766 group of clusters, age $\sim$21 Myr, the

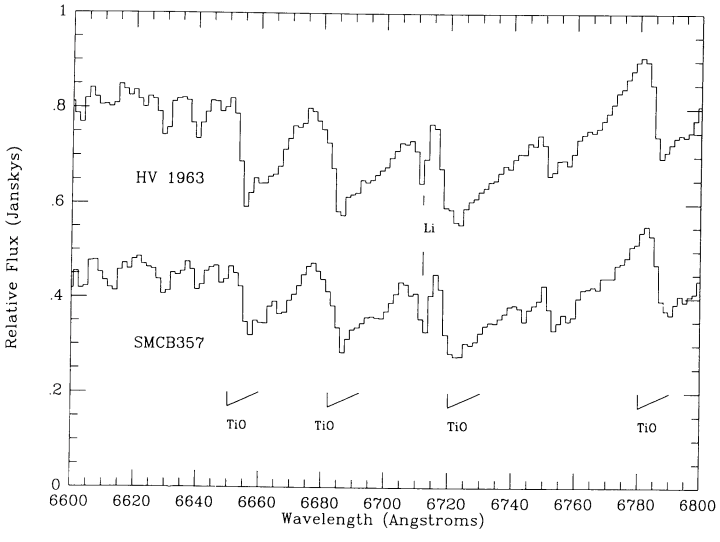


FIG. 5*a*

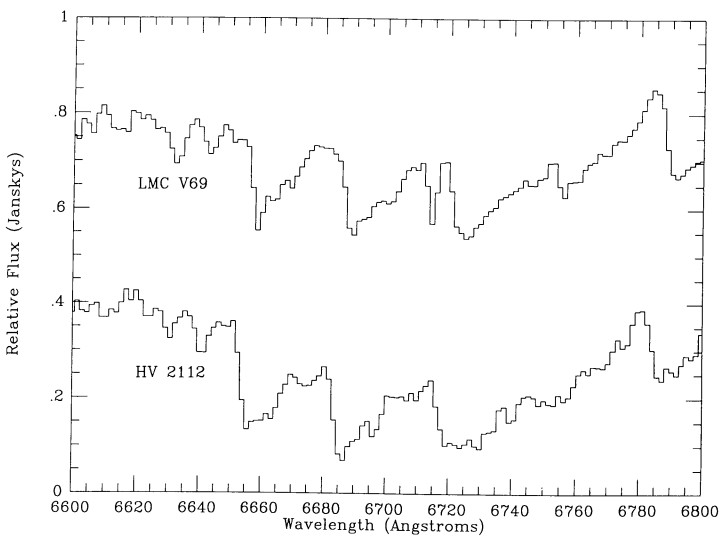


FIG. 5*b*

FIG. 5.—Lithium in luminous Magellanic Cloud AGB stars. Panel (*a*) shows our spectrum of HV 1963, which Smith and Lambert showed to have an enhanced lithium abundance evidenced by the strength of the 6707.8 doublet. This feature is clearly also present in the star SMC B357, type M4S. However, (*b*) shows that there is little evidence for abnormal abundances in HV 2112. We show our spectrum of the variable GRV 0523−6644 (No. 69 in Reid, Glass, and Catchpole 1988) to illustrate the presence of similar stars in the LMC.

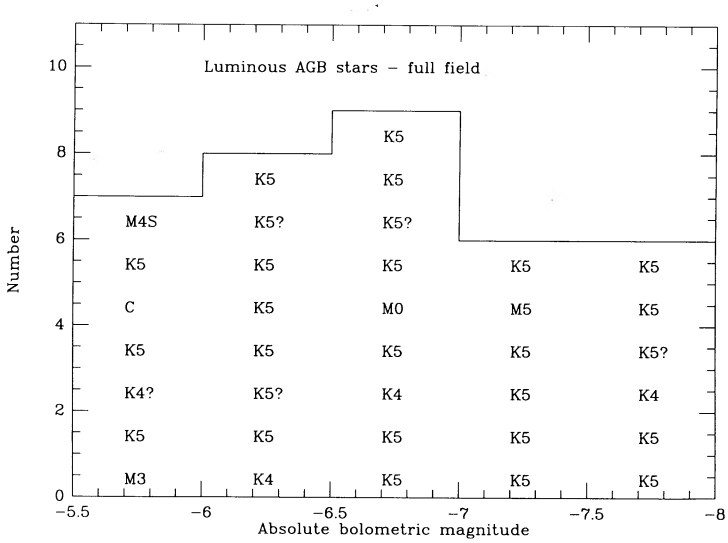


FIG. 6a

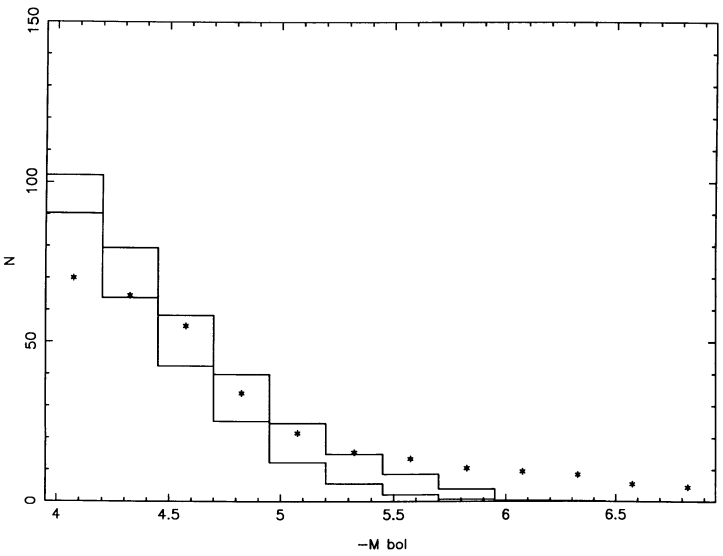


FIG. 6b

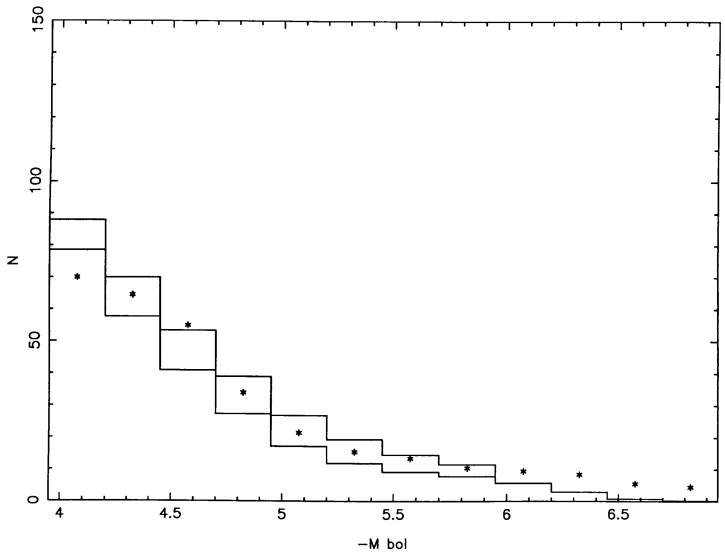


FIG. 6c

FIG. 6.—(*a*) The (spectral-type, luminosity) distribution of the brightest AGB stars. Note the absence of C stars with $M_{bol} < -6$ and the scarcity of low-temperature giants. (*b*) The luminosity function of AGB stars in the SMC compared with a constant star formation rate model. We define AGB stars as those stars with $V-I > 1.55$ and calibrate the bolometric magnitudes using the formulae given in § III. A distance modulus of 18.8 and reddening of $E_{V-I} = 0.05$ are assumed. The data are plotted as stars; the upper histogram gives the total number of AGB stars predicted by the model, while the lower histogram indicates the number of stars which have not yet undergone thermal pulses (that is, stars on the early AGB). (*c*) A comparison between the observed AGB luminosity function and a model with the star formation rate enhanced by a factor of 20 over the last $10^8$ yr.

main-sequence turnoff is at $M_v \sim -4$, and there are three red supergiants as compared with nine stars on the main sequence with luminosities in the range $-4 \leq M_v \leq -3$. In the case of the NGC 457 group, age $\sim$14 Myr and $M_v$(TO) $\sim -5$, the ratio is two red supergiants to $\sim$20 main-sequence stars. Finally, in the NGC 884 group, age $\sim$11 Myr and a turn-off luminosity of $M_v \sim -6$, there are five red supergiants as compared with 20 main-sequence stars. Combining these estimates gives a mean ratio of red supergiants to main-sequence stars of 0.2.

Comparing these results with the data obtained by RMT87 for the Shapley III region in the LMC, where the turn-off is estimated to be at $M_v \sim -4$, there are $\sim$60 stars with $-7.5 \leq M_I \leq -6$, or $M_v \sim -5.5$, and approximately 470 main-sequence stars with absolute magnitudes in the range $-3 \geq M_v \geq -4$. This gives an observed ratio of $\sim$0.13 and suggests that all of these luminous stars can be interpreted as CHB supergiants. In our SMC field we have 30 red giants with $M_I \leq -6$, or $M_v \leq -4$. Figure 7 presents the luminosity function for the main-sequence stars in our field, defined as stars with $V-I < 0.2$. The data can be represented by a power-law,

$$\phi(M_v) \propto M_v^a ,$$

where the exponent, $a$, has a value in the range 0.48–0.56. This is similar to results obtained by Freedman (1985) for M33 and other Local Group galaxies. There are 200 stars with absolute

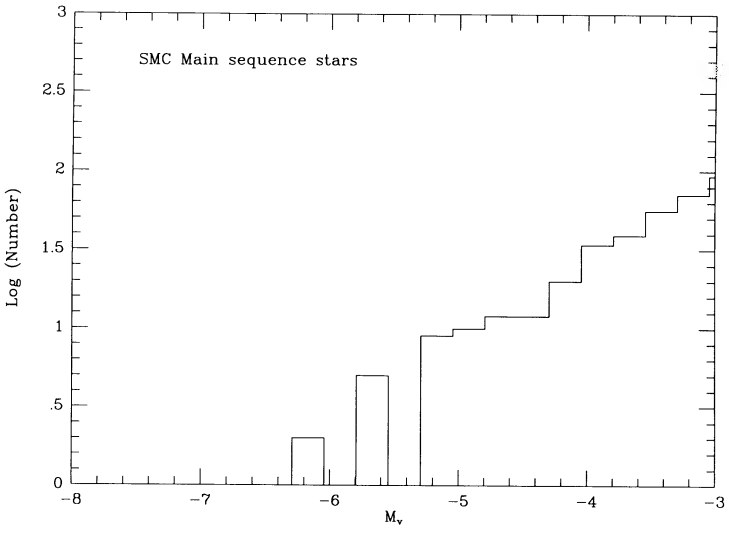


FIG. 7.—The luminosity function of main-sequence stars (defined as stars with $V-I < 0.2$) in our SMC field.

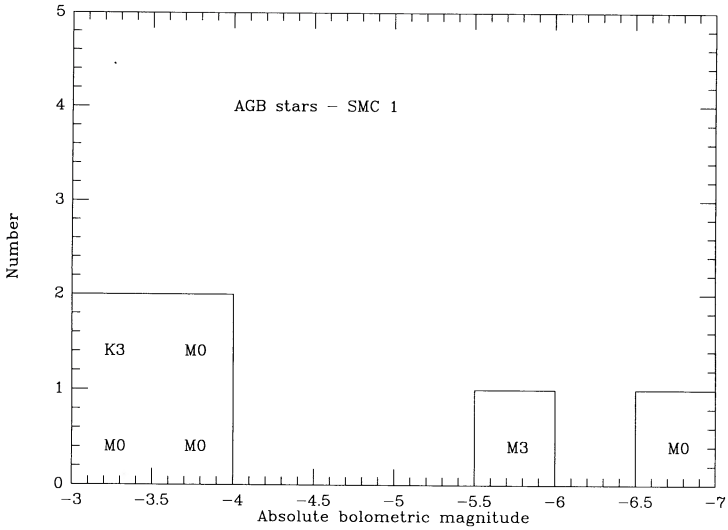


FIG. 8a

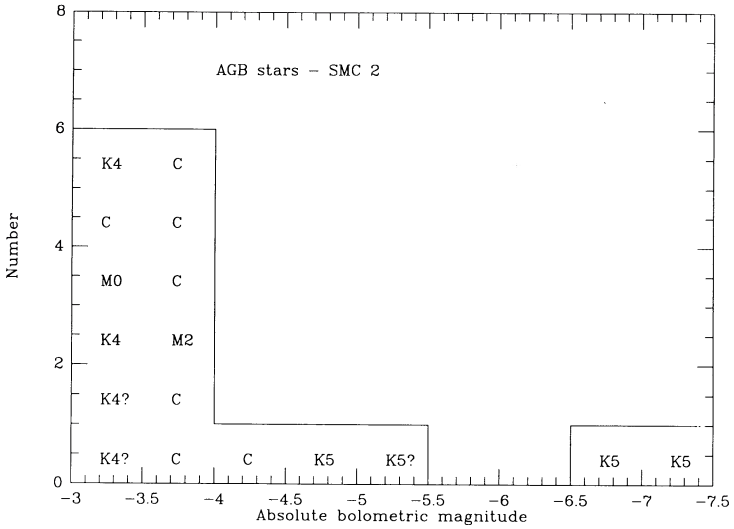


FIG. 8b

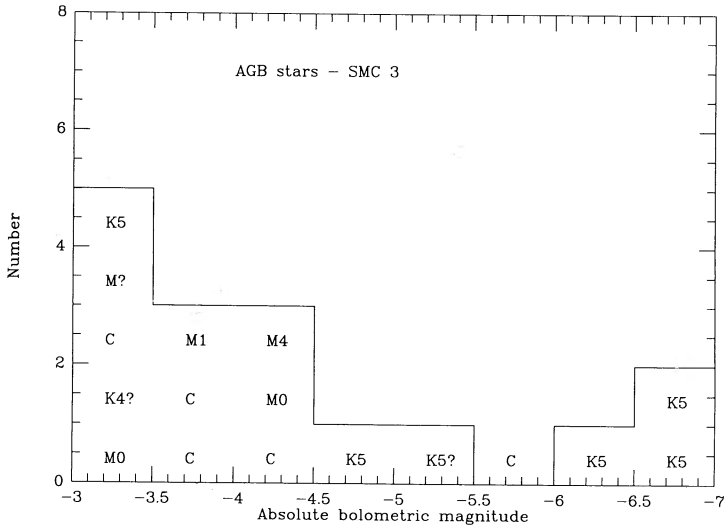


FIG. 8c

FIG. 8.—(*a*) The (spectral-type, luminosity) distribution of the AGB candidate stars observed in field 1, centered at $\alpha = 1^h8.6^m$, $\delta = -72°58'$. (*b*) Same as (*a*) for field 2, centered at $\alpha = 1^h4.15^m$, $\delta = -73°2'$. (*c*) Same as (*a*) for field 3, centered at $\alpha = 1^h4.3^m$, $\delta = -72°35'$.

visual magnitudes in the range $-3$ to $-4$, giving a red giant to main-sequence star ratio of $\sim 0.15$, consistent both with our LMC observations and with the predictions based on the open cluster data.

### *b) The Lower Luminosity AGB Stars*

The SMC giants with $M_{bol} < -5.5$ are predominantly early-type stars, with an even lower proportion of M or S stars than in the LMC. Again, as in the LMC, high-luminosity carbon stars are rare, although there are a few AGB stars which approach the theoretical limit of $M_{bol} = -7.2$. This is despite the fact that the SMC is a low abundance system, with a higher C/M ratio than the LMC (BMB80). At lower luminosities, the preponderance of C stars becomes apparent. Figure 8 shows the AGB luminosity functions for three smaller subregions within our field. There is a clear break in the number distribution at $M_{bol} \sim -4.5$, with C stars dominating the samples in two of the three fields. Considering the color-magnitude diagram, these stars lie at the tip of the RGB at $\langle I \rangle \sim 14.5$, $V-I > \sim 2$, and they are clearly relatively low-mass stars. Figure 9 compares our SMC data (including all of the AGB star candidates) with the LMC AGB luminosity function derived by Reid and Mould (1984); we have scaled the star counts in the latter by a factor of 10 to give approximate agreement at $M_{bol} \sim -4$ to $-4.5$ and take the distance modulus of the LMC as 18.4 rather than 18.7. The agreement in shape between the two data sets is striking. The larger number of stars in the SMC sample with the $M_{bol} < -5.5$ may reflect a higher proportion of young supergiants, since the LMC (North) field encompasses few regions of recent star formation. Taking $M_{bol} = -4.75$ as the peak luminosity of the AGB for this population implies an age of $\geq 2$–3 Gyr (Reid and Mould 1985, Fig. 7).

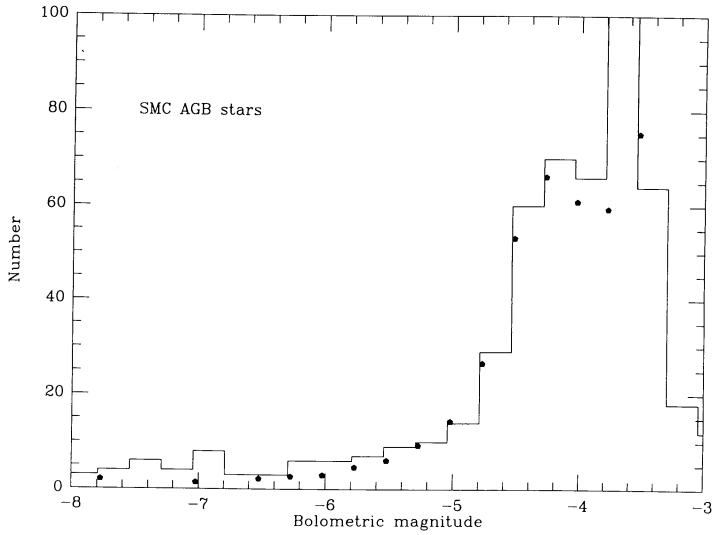


FIG. 9.—A comparison between the photometrically derived AGB star luminosity functions in LMC (*solid points*) and SMC (*histogram*). The former data are taken from Reid and Mould (1984), taking the LMC distance modulus as 18.4 (rather than the value of 18.7 adopted in that paper) and scaling the number counts by a factor of 10.

One of the three subregions studied, SMC 1, is unusual in having no C stars brighter than $M_{bol} = -3.0$. This field is in what we have termed the "halo" region of our field, and there are only six AGB candidates, four in the lower luminosity group. However, the C:M ratios in the other two fields ($M_{bol} > -4.5$) are 7:5 and 4:5, respectively, so the probability of this absence of C stars being a chance occurrence is less than 5%. If we consider the color-magnitude diagram for this region (Fig. 1*a*), there are significantly fewer stars with $V-I > 1.8$, confirming the lower fraction of C stars. Lying in the outer regions of the SMC, it is possible that the stellar population in this field is sufficiently old that the evolved stars are not massive enough to dredge up carbon (Iben and Renzini 1983).

## V. THE DEPTH OF THE SMC

Since McGee and Newton's (1981) H I observations, it has been clear that the SMC has a complex geometry, with two particularly prominent velocity systems at $V_\odot \sim 140$ km s$^{-1}$ (component *L*) and $V_\odot \sim 190$ km s$^{-1}$ (component H). This complex velocity field is generally believed to be a result of gravitational interactions between the SMC and both the LMC and the Galaxy (Murai and Fujimoto 1980). Various authors, in particular Mathewson, Ford, Visvanathan (1986, 1988), have interpreted the bifurcated velocity distribution as indicating the presence of two SMC fragments at different distances. Estimates of the separation between these systems range from more than 20 kpc (MFV88) to as little as 4 kpc (Welch *et al.* 1987, analyzing a small sample of Cepheids). Most recently, Martin, Maurice, and Lequeux (1989) have reviewed the available data. They identify four main velocity systems in the H I gas, adding lower (VL) and higher (VH) velocity components to the two identified by MFV86, and while they find evidence that component H lies in front of component L, they conclude that most of the young stars in the SMC are within 10 kpc depth, although there may be a greater range in distance in the south-west region of the Galaxy.

Our data cover a part of the SMC where gas from both the H and L complexes is present (see Martin, Maurice, and Lequeux, Figs. 4B and 4C). Thus we can use both the morphology of the color-magnitude diagram and the radial velocity distribution (Fig. 10) to investigate the depth of the SMC within our field. The lower histogram includes only oxygen-rich (K, M, S) stars, while the upper adds C stars. The two velocity systems are clearly present amongst the giants that we have observed, with the bimodal distribution peaking at $V_\odot \sim 155$ km s$^{-1}$ ($V_{GSR} \sim -10$ km s$^{-1}$) and $V_\odot \sim 195$ km s$^{-1}$ ($V_{GSR} \sim +30$ km s$^{-1}$), where $V_{GSR}$ is the velocity with respect to the Galactic center computed using the formula given by Martin, Maurice, and Lequeux. (The effects of galactic rotation are small within the 0.8 deg$^2$ area covered by our observations.) The higher velocity system has a slightly narrower distribution. Both C and K/M stars show the same distribution, with roughly equal numbers in the two groups. This is in contrast to the more extensive survey of SMC carbon stars by Azzopardi, Suntzeff, and Hardy (1989), where there is little evidence of bimodality. This probably stems from the fact that the latter survey covers a much larger fraction of the SMC, including regions where the H I shows a single-peaked velocity distribution.

However, while our radial velocity data show the two velocity systems, as we have already noted in § II, the SMC red giant branch is very narrow in the ($I$, [$V-I$]) color-magnitude diagram, with most of the stars lying within only $\sim \pm 0.1$ mag about the fiducial line, and at least part of the scatter is due to abundance variations. A dispersion of 0.1 mag corresponds to only $\pm 2.5$ kpc in distance for $m - M = 18.8$. Hatzidimitriou, Hawkins, and Gyldenkerne (1989) have undertaken a similar study of the outer regions of the SMC, using photographic photometry of the stars in the red clump to probe the depth of the old stellar population of the SMC as a function of position. Over much of the SMC, their data agree with our results in this field, showing little dispersion in distance. However, in the northeast section of the SMC, the red clump broadens in magnitude, which they interpret as a distortion of the older stellar population in the direction of the LMC.

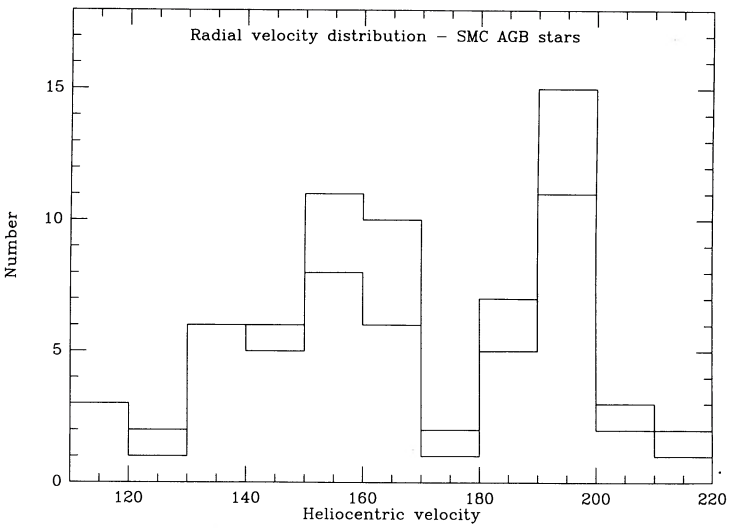


FIG. 10.—The velocity distribution of the SMC AGB stars. The heliocentric velocities plotted can be converted to galactocentric values by subtracting 165 km s$^{-1}$. The lower histogram includes all save the carbon stars, which are added to give the upper histogram.

The referee has pointed out that the velocity data, both H I and our observations, refer to relatively young components, while the giant branch stars are older, with ages $\geq 2$ Gyr. Nonetheless, our data show that if the bimodal velocity distribution reflects a bimodal distance distribution, the bimodality is confined largely to the younger objects, at least within this field. This suggests a dissipative collision, with star formation triggered in the disturbed gas, rather than a purely gravitational interaction, with most of the mass of the SMC (as characterized by the distribution of the older population) remaining in a relatively compact, if disturbed, system.

## VI. CONCLUSIONS

We have used a $V$- and $I$-band photographic survey to identify a sample of red giant stars within a 0.8 deg$^2$ region of the SMC. We have obtained spectroscopic observations of all AGB candidates with $M_{bol} < -5.5$ within this field, as well as surveying three samples extending to $M_{bol} = -3$ within three smaller regions. As in the LMC, there are very few luminous AGB stars, with the brightest carbon star having a luminosity of $M_{bol} = -5.7$. Indeed, the luminosity function in this field is very similar in shape to that of the outer regions of the LMC, suggesting a very similar star formation history. Finally, our radial velocity measurements clearly show the bimodal velocity structure evident in H I maps of the SMC, but the narrowness of the giant branch in our color-magnitude diagrams argues against this spread in velocity reflecting a line-of-sight depth of more than 5 kpc in the old stellar population.

REFERENCES


Azzopardi, M., Suntzeff, N. B., and Hardy, E. 1989, *Ap. J.*, **344**, 210.
Azzopardi, M., and Vigneau, J. 1975, *Astr. Ap.*, **22**, 285.
Bessell, M. S. 1985, in *IAU Symposium 108, The Structure and Evolution of the Magellanic Clouds*, ed. S. van den Bergh and K. S. de Boer (Dordrecht: Reidel), p. 171.
Bessell, M. S., and Wood, P. R. 1984, *Pub. A.S.P.*, **96**, 247.
Blanco, V. M., and McCarthy, M. F. 1983, *A.J.*, **88**, 1442.
Blanco, V. M., McCarthy, M. F., and Blanco, B. 1980, *Ap. J.*, **242**, 938.
Butler, D., Demarque, P., and Smith, H. A. 1982, *Ap. J.*, **257**, 592.
Da Costa, G. S., and Armandroff, T. 1990, preprint.
Da Costa, G. S., and Mould, J. R. 1986, *Ap. J.*, **305**, 214.
Freedman, W. 1985, *Ap. J.*, **299**, 74.
Graham, J. A. 1975, *Pub. A.S.P.*, **87**, 641.
———. 1982, *Pub. A.S.P.*, **94**, 244.
Hatzidimitriou, D., Hawkins, M. R. S., and Gyldenkerne, K. 1989, *M.N.R.A.S.*, **241**, 667.
Iben, I., and Renzini, A. 1982, *Ap. J.* (*Letters*), **259**, L79.
———. 1983, *Ann. Rev. Astr. Ap.*, **21**, 271.
Lattanzio, J. C. 1987, in *ACS Symposium on the Origin and Distribution of the Elements*, ed. G. J. Mathews (Singapore: World Scientific), p. 55.
Maeder, A. 1981, *Astr. Ap.*, **102**, 401.
Martin, N., Maurice, E., and Lequeux, J. 1989, *Astr. Ap.*, **215**, 219.
McGee, R. X., and Newton, L. M. 1981, *Proc. Astr. Soc. Australia*, **4**, 189.
Mathewson, D. S., Ford, V. L., and Visvanathan, N. 1986, *Ap. J.*, **301**, 664.
———. 1988, *Ap. J.*, **333**, 617.
Mermilliod, J.-C., and Maeder, A. 1986, *Astr. Ap.*, **158**, 45.
Mould, J. R., and Aaronson, M. 1982, *Ap. J.*, **263**, 629.
———. 1986, *Ap. J.*, **303**, 10.
Mould, J. R., Da Costa, G. S., and Crawford, M. D. 1984, *Ap. J.*, **280**, 595.
Mould, J. R., Kristian, J., and Da Costa, G. S. 1983, *Ap. J.*, **270**, 471.
Mould, J. R., and Reid, I. N. 1987, *Ap. J.*, **321**, 156.
Murai, T., and Fujimoto, M. 1980, *Pub. Astr. Soc. Japan*, **32**, 581.
Reid, I. N. 1987, *M.N.R.A.S.*, **225**, 873.
Reid, I. N., Glass, I. S., and Catchpole, R. M. 1988, *M.N.R.A.S.*, **232**, 53.
Reid, I. N., and Mould, J. R. 1984, *Ap. J.*, **284**, 98.
———. 1985, *Ap. J.*, **299**, 236.
Reid, I. N., Mould, J. R., and Thompson, I. 1987, *Ap. J.*, **323**, 433 (RMT87).
Reid, I. N., and Strugnell, P. 1986, *M.N.R.A.S.*, **221**, 887.
Reid, I. N., Tinney, C. G., and Mould, J. R. 1990, *Ap. J.*, **348**, 98 (RTM90).
Schechter, P. 1988, *A Guide to the Modular Spectrograph* (Washington, DC: Observatories of the Carnegie Institute of Washington).
Smith, V. V., and Lambert, D. L. 1989, *Ap. J.* (*Letters*), **345**, L75.
Stone, R. P. S., and Baldwin, J. A. 1983, *M.N.R.A.S.*, **204**, 347.
Suntzeff, N. B., Friel, E., Klemola, A., Kraft, R. P., and Graham, J. A. 1986, *A.J.*, **91**, 275.
Welch, D. L., McLaren, R. A., Madore, B. F., and McAlary, C. W. 1987, *Ap. J.*, **321**, 162.
Wood, P. R., Bessell, M. S., and Fox, M. W. 1983, *Ap. J.*, **272**, 99 (WBF).


JEREMY MOULD and NEILL REID: Laboratory of Astrophysics, 105-24, California Institute of Technology, Pasadena, CA 91125